Rounded Corners in Microwave High-Power Filters and Other Components*

SEYMOUR B. COHN†, FELLOW, IRE

Summary—Microwave high-power filters must be operated with internal air pressures of at least one atmosphere, or with a good vacuum. Pressures between these extremes result in reduced power-handling ability. The breakdown processes for both high air pressure and vacuum are discussed, and it is made clear that any sharp corner on which the electric field would concentrate must be rounded if high-power operation is to be achieved. For good results in vacuum operation, the surfaces must be especially smooth and free of contamination, while in high-pressure operation, minor irregularities are less important.

Various high-power filter configurations of importance are described, and the structural corners at which electric-field concentrations occur are pointed out. A number of simplified geometries are then shown that can represent the essential portions of the practical structures with sufficient accuracy for ordinary purposes. Formulas and graphs for these simplified geometries are presented that give the ratio of the maximum electric field strength on the boundary to a uniform reference field strength at a point sufficiently removed from the corner. In some cases, the boundary curve is an approximation to a circular arc, while in other cases a boundary shape is derived such that the electric field strength along the curve is constant. These constant-field-strength boundaries are optimum shapes from the standpoint of power-handling ability.

I. Introduction

THE maximum allowable power flow in high-power filters or other components is limited by ionization breakdown in regions of high electric-field concentration. The critical value of electric field above which breakdown occurs depends upon a number of interdependent factors: 1) the composition and pressure of the air or other gas filling the device; 2) the signal frequency; 3) the size and shape of the region over which the electric field approaches its maximum concentration; 4) the presence of nearby conducting surfaces, their shapes, and their spacings; and 5) the pulse length, shape, and repetition frequency.

The breakdown process as a function of the above parameters has been analyzed by Gould.[1] His work shows that for usual sizes of uniform waveguides and coaxial lines operated near standard-atmosphere air pressure, the ratio of the peak RF electric field strength at breakdown in volts per centimeter to the pressure in atmospheres is approximately independent of factors 2)–5), and is near to the previously accepted value of 29,000 volts/cm/unit pressure in atmospheres.[2] Gould has not considered more complex geometries, but his data for coaxial lines indicate that this figure would hold approximately for rounded-corner radii as small as 1 mm at one atmosphere pressure, with the breakdown field strength being higher for smaller radii or smaller pressure. (For constant error, radius times pressure is a constant.) As the pressure is decreased below one atmosphere, factors 2)–5) begin to have much stronger effects. However, since a high-power filter would usually be operated with at least one atmosphere of pressure, it appears a reasonably good approximation to treat the value of 29,000 volts/cm/atmosphere as a constant. Fortunately, this is a conservative approximation, since the effect of factors 2)–5) is to raise rather than lower the breakdown field strength.

At a pressure of the order of one millimeter of mercury, the breakdown field strength as a function of pressure passes through a minimum. At lower pressures, the breakdown field strength increases rapidly. At pressures lower than about 10^{-6} mm Hg, corresponding to a good vacuum, ionization of the remaining air molecules is no longer important and another mechanism of breakdown becomes limiting. Much less is known about RF breakdown in vacuum than at high pressures. However, current evidence indicates that the RF breakdown mechanism in vacuum is *field emission* of electrons from conducting surfaces. Field emission requires field strengths of the order of megavolts per cm.[3] Such field strengths may develop at minute irregularities, thus initiating breakdown, even when the macroscopic field strength is much lower. Because of this it is extremely important that the surface be smooth and free of contamination.

It has thus been established that the attainment of prespecified values of electric field strength will result in breakdown of high-power microwave filters at high pressures. In vacuo, it is not certain whether a definite breakdown field strength can be prespecified, but nevertheless the breakdown power can certainly be increased by minimizing electric-field concentrations. Thus either in high pressure or in vacuo, any edges at which the electric field may concentrate should be rounded. As an aid in determining the degree of round-

* Received by the PGMTT, March, 7, 1961; revised manuscript received, May 25, 1961. This work was performed at Stanford Res. Inst., Menlo Park, Calif., under the support of the Rome Air Dev. Ctr., under Contract No. AF 30(602)-1998.

† Rantec Corp., Calabasas, Calif.

[1] L. Gould, "Handbook on Breakdown of Air in Waveguide Systems," Microwave Associates, Inc., Burlington, Mass. Rept. on Contract Nobsr 63295; April, 1956.
Also, L. Gould and L. W. Roberts, "Breakdown of air at microwave frequencies," *J. Appl. Phys.*, vol. 27, pp. 1162–1170; April, 1956.

[2] H. A. Wheeler, "Nomogram for Some Limitations on High-Frequency Voltage Breakdown in Air," Wheeler Labs., Inc., Monograph No. 17; May, 1953.

[3] W. S. Boyle, P. Kisliuk, and L. H. Germer, "Electrical breakdown in high vacuum," *J. Appl. Phys.*, vol. 26, pp. 720–725; June, 1955.

ing necessary, a number of rounded-corner geometries important in microwave-filter structures have been analyzed by conformal-transformation methods, and the results are given in this paper. For each geometry considered, the maximum field is related to a reference field at a sufficient distance from the rounded edge that the reference field will be essentially uniform. This information will enable filter designers to relate the maximum field strength occurring in a given filter to the power passing through it. The breakdown value of power may then be determined in the case of high air pressure by setting this maximum field strength equal to approximately 29,000 volts/cm multiplied by the pressure in atmospheres. A safety factor should of course be applied to the calculated breakdown power in order to arrive at a safe power rating for the filter.

Another phenomenon which can, under special circumstances, reduce the power transmitted through an evacuated high-power filter is called *multipactor*.[4] Multipactor is a resonant secondary-emission process in an evacuated region that occurs when an electron under the action of an RF electric field has a time of transit between opposite walls of the region that equals approximately one-half the period of an RF cycle. Limited evidence available to this author indicates that in high-power filters utilizing low-Q elements, multipactor would ordinarily absorb no more than a few watts of power, and hence would not greatly affect performance. If high-Q elements are used however, the loss may be large.

II. Typical High-Power Filter Configurations

Fig. 1 shows simplified sketches of a number of basic high-power filter structures in which electric-field concentration occurs at corners. At all outside corners in the E plane, such as those marked A, the field strength would approach infinity if the radius of the corner were made to approach zero. At all inside sharp corners, such as those marked B, the field strength is zero and is hence no problem. Fig. 1(a) is typical of the corrugated, or varying-impedance filter.[5,6] Fig. 1(b) is a modification of Fig. 1(a), in which the angle of the corner is changed to decrease the field concentration.[7] Figs. 1(c) and 1(d) are leaky wall filters, in which slots in the broad walls of the main waveguide open into

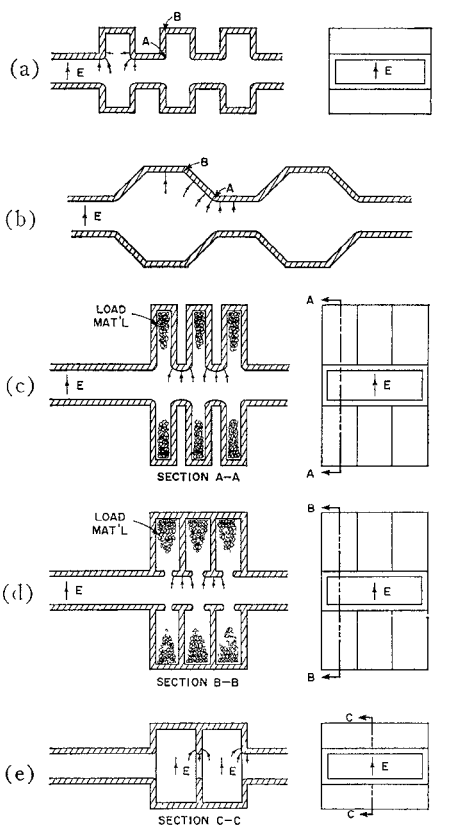

Fig. 1—Typical rounded-corner configurations in high-power filters.

secondary waveguides of higher cutoff frequency.[8–10] Fig. 1(e) is a coupled-cavity filter with rounded edges at the apertures.[8]

Rigorous solutions of the structures in Fig. 1 would be virtually impossible to achieve. However, the solutions for a number of simpler cases shown in Fig. 2 have been obtained that may be applied to the actual filter structures with accuracy sufficient for practical purposes. The two most important assumptions are: 1) the rounded corner geometry may be considered to be composed of infinite cylindrical surfaces, so that the solution for a single two-dimensional cross section is sufficient, and 2) the essential portions of the cross section are small compared to a wavelength, so that the field distribution in those regions may be considered to be very nearly a static field distribution. The first assumption applies exactly to cases like Fig. 1(a) and 1(b), and with fair accuracy to cases like Fig. 1(c)–1(e). The second assumption will usually apply with good accuracy in the pass band of these filters, even though

[4] W. G. Abraham, "Interactions of Electrons and Fields of Cavity Resonators," Ph.D. dissertation, Dept. of Elec. Engrg., Stanford Univ., Stanford, Calif.; 1950.

[5] S. B. Cohn, "Design relations for the wide-band waveguide filter," Proc, IRE, vol. 38, pp. 799–803; July, 1950.

[6] B. M. Schiffman and S. B. Cohn, "Wide-Stop-Band Waveguide Filters," presented at the 1959 PGMTT Natl. Symp., Harvard Univ., Cambridge, Mass.; June 1, 1959.

Also see S. B. Cohn, *et al.*, "Design Criteria for Microwave Filters and Coupling Structures," Stanford Res. Inst., Menlo Park, Calif., Tech. Rept. No. 2, Contract No. DA36-039-SC-74862; June, 1958.

[7] J. H. Vogelman, "High-power microwave filters," IRE Trans. on Microwave Theory and Techniqes, vol. MTT-6, pp. 429–439; October, 1958.

[8] S. B. Cohn, "Design considerations for high-power microwave filters," IRE Trans. on Microwave Theory and Techniques, vol. MTT-7, pp. 149–153; January, 1959.

[9] V. Met, "Absorptive filters for microwave harmonic power," Proc. IRE, vol. 47, pp. 1762–1769; October, 1959.

[10] V. G. Price, R. H. Stone, and V. Met, "Harmonic suppression by leaky-wall waveguide filter," 1959 IRE WESCON Convention Record, pt. 1, pp. 112–118.

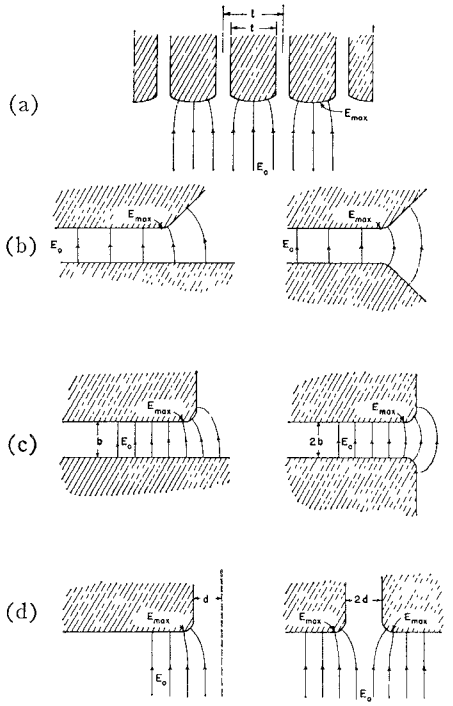

Fig. 2—Two-dimensional geometries considered in this paper.

the over-all waveguide or cavity dimensions are large parts of a wavelength.

The two-dimensional geometries considered in this paper are shown in Fig. 2. The angular designation applied to each corner in Fig. 2 indicates the change in direction of a tangent line as it is moved around the corner. The array of 180-degree rounded corners of Fig. 2(a) has most direct application to the leaky-wall filters of Fig. 1(c) and 1(d). The individual conductors of the array are assumed to be at the same potential. Their center-to-center spacings are assumed to be sufficiently smaller than the spacing to any other conducting surface that the field well below the array of corners may be considered uniform, and equal to a reference value E_0. The 45-degree rounded corner of Fig. 2(b) applies to the varying-impedance filter of Fig. 1(b). By image arguments, the unsymmetrical and symmetrical forms of the 45-degree corner may, of course, be shown to have identical solutions. In this case, the reference field is the uniform field E_0 in the parallel-plane region at a point sufficiently removed from the corner. The 90-degree corner near an electric wall, Fig. 2(c), applies to varying-impedance filter structures when the spacing between the broad walls of the main waveguide is small compared to the width of the slots. The 90-degree rounded corner near a magnetic wall, Fig. 2(d), may be applied to slots in the broad wall of a waveguide when the RF voltage across the slot is relatively small. This would usually be true in the pass band for the leaky-wall filters of Figs. 1(c) and 1(d), but not usually in the pass band of the varying-impedance filter of Fig. 1(a). In that case, when the dimensions are about as shown in the figure, the field in the vicinity of the slot opening may be obtained to a good approximation by superimposing the field distributions of Figs. 2(c) and 2(d).

The coupled-cavity filter of Fig. 1(e) is an example of a more complex structure to which the rounded-corner data of this paper may be applied. The maximum electric field strength will occur in the central longitudinal E plane of the filter. In the absence of the coupling apertures, the field would be greatest at the centers of the cavities, and zero along their vertical sides. In the presence of the coupling apertures, however, there will be electric field concentrations along the top and bottom edges of the apertures that could exceed the field strength at the cavity centers unless the edges are sufficiently rounded. The maximum field strength at the input and output couplings of Fig. 1(e) may be determined from the solution for Fig. 2(c), and that at the central coupling from the solution for Fig. 2(a), with $t/l \ll 1$.

III. Array of 180-Degree Rounded Corners

In the case of an array of 180-degree rounded corners, a method of analysis due to Wheeler[11] has made possible the derivation of the curved-boundary shape upon which the E field is constant (see Part A of Appendix). Figs. 3 and 4 show to scale the resulting boundary shapes for different values of plate thickness t to center-to-center spacing l. It is seen that the radius of curvature varies greatly over each curved portion of the boundary, being relatively large at the center point and decreasing toward the ends. This variation in curvature is necessary in order to maintain constant field strength over the curved boundary. On the straight, vertical portions of the boundary, the field drops off rapidly from the corner. If the curved boundary had any other shape, the field would be nonuniform, attaining in some regions values higher than the constant value occurring on the boundaries of Figs. 3 and 4. Consequently, the boundary shapes in these figures are particularly significant for the design of high-power filters requiring this basic configuration.

The constant field strength E_{max} turns out to be very simply related to the uniform field E_0 well below the array, as follows:

$$\frac{E_{max}}{E_0} = \sqrt{\frac{l}{t}}. \tag{1}$$

The square-root relationship makes E_{max}/E_0 increase slowly as t/l is decreased. For example, if t/l equals 0.5, E_{max}/E_0 will equal 1.414, and if t/l equals 0.1, E_{max}/E_0 will equal 3.16. Points x, y on the curved

[11] H. A. Wheeler, "Conformal Mapping of Rounded Polygons by a Wave-Filter Analog," Wheeler Labs., Inc., Great Neck, N. Y., Rept. No. 667; August 8, 1955.

boundary may be computed by means of the following parametric equations:

$$x = \frac{l-t}{2\pi}\left[p \tan^{-1}(p \tan \phi) - \phi\right] \tag{2}$$

$$y = \frac{l-t}{4\pi} \ln\left[1 + (p^2 - 1)\sin^2 \phi\right], \tag{3}$$

where $p=(1+t/l)/(1-t/l)$, and where ϕ is an independent variable. The co-ordinate system is shown in Fig. 5. As ϕ is increased from $-\pi/2$ to $\pi/2$, the point x, y moves from the left end of the curve to the right end, resulting in a curve that is a symmetrical function of ϕ. The coordinates of the end points are

$$\frac{x_1}{t} = \pm\frac{1}{2}, \qquad \frac{y_1}{t} = \frac{1}{2\pi}\,\frac{1-t/l}{t/l}\ln\frac{1+t/l}{1-t/l}. \tag{4}$$

The value of y_1/t decreases from 0.318 for $t/l=0$ to 0 for $t/l=1$, which results in the curve shapes being more flattened for the larger t/l values, as may be seen in Fig. 4.

There are two special cases of constant-field-strength boundaries that may be derived from (2)–(4). The first is that of an isolated plate with rounded edge, obtained when $l/t\to\infty$. The curve for this case, which was computed previously by Wheeler,[11] is plotted in Fig. 6. The end points are $x_1=\pm t/2$ and $y_1=0.318t$. This curve may be used in other situations than that of Fig. 6 as an approximation to the ideal curve, if the edge of a plate is removed from any other boundary surface by a distance equal to at least several plate thicknesses.

The other special case is that of an isolated slot with rounded edges where the two sides of the slot are at the same potential. The boundary shape, obtained when $t/l\to 1$, is shown in Fig. 7. It is seen that the curve falls monotonically to the left, but approaches zero slope as $x\to-\infty$. Eq. (1) shows that the field strength on the curved boundary is equal to the uniform field strength far below it. However, because of its infinite extent, the boundary must in practice be altered at some point, in which case a somewhat greater maximum field strength will occur.

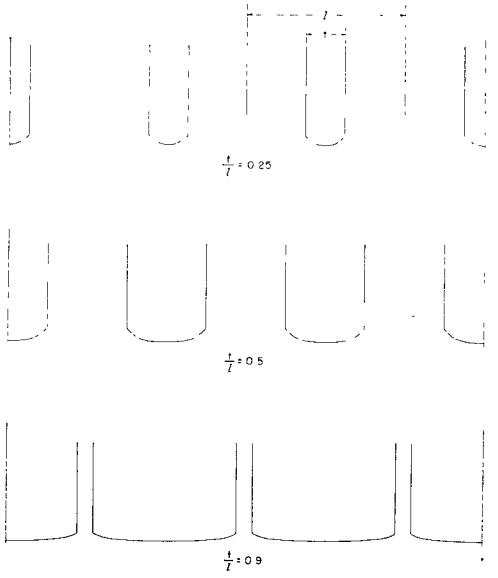

Fig. 3—Arrays of rounded 180-degree corners shaped for constant electric field.

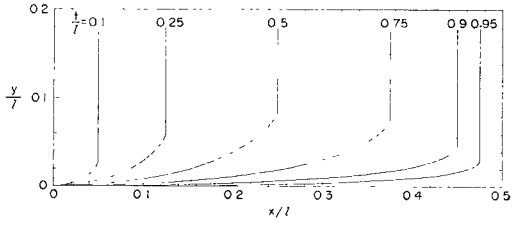

Fig. 4—Shapes of rounded 180-degree corners for various values of t/l.

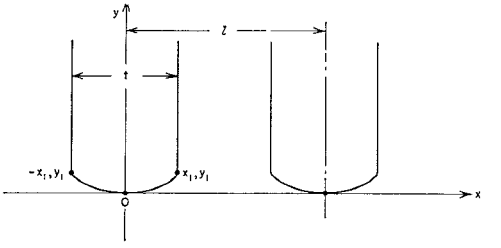

Fig. 5—Coordinate system for array of 180-degree corners.

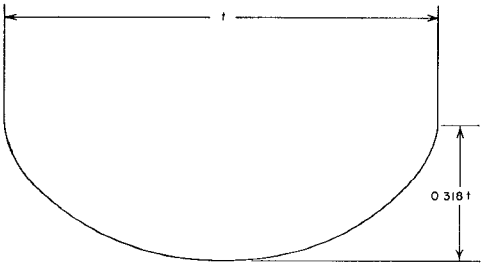

Fig. 6—Isolated rounded 180-degree corner plotted to scale.

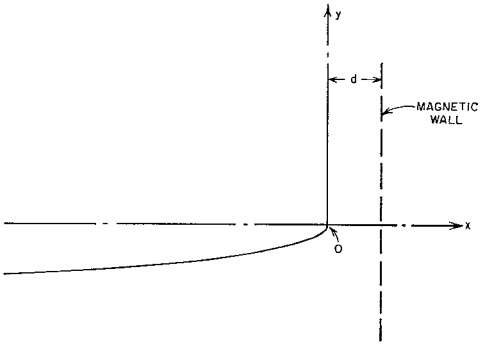

Fig. 7—Limiting case of rounded 180-degree corner for $t/l\to 1$.

IV. Rounded 90-Degree Corner Near Electric Wall

Fig. 2(c) shows a rounded 90-degree corner near an electric wall, and its symmetrical equivalent. Two curved-boundary shapes are of interest: 1) a circular arc, and 2) a shape resulting in constant field strength on the rounded surface.

A. Approximate Circular Boundary

It is not feasible to solve exactly the case of a 90-degree circular-arc corner, but a solution has been obtained for a shape that is a good approximation to a circular arc.[12–14] The actual curved boundary obtained in this case is shown in Fig. 8 for two values of r/b, where r and b are defined in the figure. These boundaries were plotted with the aid of formulas given by Weber.[15] (Note, however, that Weber's plot of one of the boundaries[16] is grossly inaccurate.) The formula for the ratio of E_{max}/E_0 as a function of r/b is also given by Weber, and is plotted in Fig. 9. For example, $E_{max}/E_0 = 1.40$ at $r/b = 0.6$. Thus, in a rectangular waveguide containing such a corner, breakdown will occur at about half the breakdown power of the uniform waveguide itself.

An abrupt step in height of a waveguide, or in diameter of a coaxial line, has an equivalent circuit consisting simply of a shunt capacitive susceptance at reference planes coinciding with the step itself. Graphical data have been published giving the value of this susceptance for sharp-corner rectangular-waveguide and coaxial-line configurations.[17,18] If the corner is rounded, the discontinuity susceptance will be less than that of a sharp corner. A formula for the change in susceptance, ΔB, was previously derived by this author[19] for the approximate circular-arc case. The resulting plot of ΔB versus r/b is given in Fig. 10 for a step in height in rectangular waveguide. The total shunt susceptance of the rounded step is

$$B = B\big|_{r=0} + \Delta B, \tag{5}$$

where $B\big|_{r=0}$ is the susceptance of a sharp step.[16] Note that ΔB is a negative quantity, and hence B is smaller than $B\big|_{r=0}$. Rounding of the corner also results in an

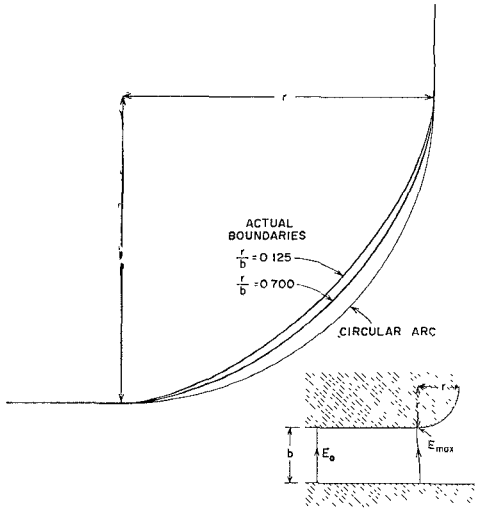

Fig. 8—Actual shape of approximately circular, 90-degree rounded corner near an electric wall.

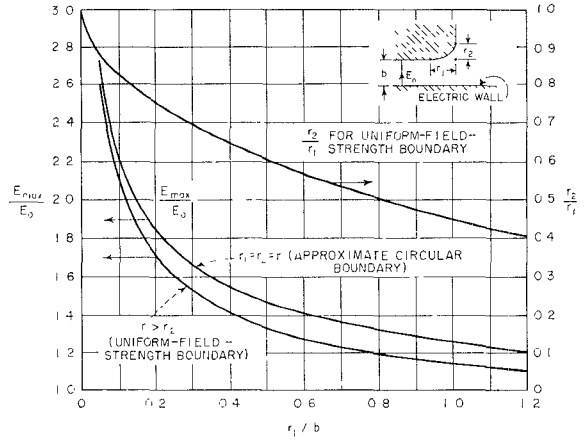

Fig. 9—Plot of E_{max}/E_0 for rounded 90-degree corner near an electric wall; also, r_2/r_1 for a uniform-field-strength boundary.

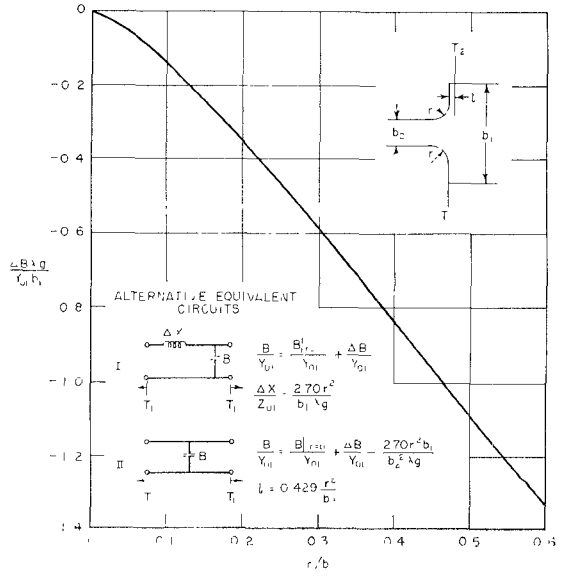

Fig. 10—Capacitive susceptance correction and equivalent circuits for rounded step in waveguide.

[12] L. Dreyfus, "Zur Berechnung von Durchslags und Überschlagsspannung," *Arch. Electrotech.*, vol. 13, p. 131; 1924.
[13] J. D. Cockcroft, "The effect of curved boundaries on the distribution of electrical stress round corners," *J. IEE*, vol. 66, pp. 385–409; 1928.
[14] E. Weber, "Electromagnetic Fields," John Wiley and Sons, Inc., New York, N. Y., vol. I, pp. 373–377; 1950.
[15] *Ibid.*, p. 374.
[16] *Ibid.*, p. 376.
[17] N. Marcuvitz, "Waveguide Handbook," McGraw-Hill Book Co., Inc., New York, N. Y., Rad. Lab. Series, vol. 10, pp. 307–312; 1951.
[18] J. R Whinnery, H. W. Jamieson, and T. E. Robbins, "Coaxial-line discontinuities," Proc. IRE, vol. 32, pp. 695–709; November, 1944.
[19] S. B. Cohn, unpublished note; March, 1958.

increase in stored magnetic energy. This may be taken account of by adding a series inductive element in the equivalent circuit at the reference plane of the step, or by a shift of one of the reference planes and modification of B. These alternative equivalent circuits are shown in Fig. 10. Values of ΔB taken from the curve in Fig. 10 will be accurate as long as r is sufficiently small compared to the dimension $(b_1-b_2)/2$. Good results should be expected for r as large as one half that dimension. It is also necessary that $\Delta X/Z_{02}$ be small; *e.g.*, less than 0.3 should suffice.

B. Constant-Field-Strength Boundary

A solution in the case of a rounded 90-degree corner near an electric wall has been obtained yielding the boundary shape having uniform field strength on the curved arc.[12,13] Cockroft[13] gives formulas from which this boundary shape may be plotted, and shows in his Fig. 19 one such boundary drawn to scale. The shape of the boundary is very much like that of Fig. 8, but compressed in height. The plot of E_{max}/E_0 versus r_1/b for this case is included in Fig. 9. Also plotted is the ratio of r_1 and r_2, the dimensions that define the horizontal and vertical extent of the curved boundary. As should be expected, the E_{max}/E_0 curve for the uniform-field-strength case falls below that for the approximate circular-arc case. The two cases coalesce as r_1/b approaches zero.

V. Rounded 90-Degree Corner Near Magnetic Wall

A rounded 90-degree corner near a magnetic wall is shown in Fig. 2(d), along with its symmetrical equivalent. As in the case of an adjacent electric wall, Section IV, two curved-boundary shapes are of particular interest: 1) a circular arc, and 2) the shape resulting in constant field strength on the rounded surface.

A. Approximate Circular Boundary

The approximate-circular-arc solution discussed in Section IV-A has been modified to apply to an adjacent magnetic wall (see Part B of Appendix). The boundary shape is exactly the same as in Section IV-A, and hence Fig. 8 applies to the magnetic-wall case as well as to the electric-wall case if $r/d=r/b$. For the adjacent magnetic wall, the ratio of the maximum field strength on the boundary to the distant uniform field strength was found to be

$$\frac{E_{max}}{E_0} = (1+\lambda)\sqrt{1+p}, \tag{6}$$

where λ and p are parameters plotted by Weber[14] in his Fig. 28.8. Eq. (6) is plotted in Fig. 11. The maximum-field-strength point occurs at the end of the curved boundary farthest from the magnetic wall.

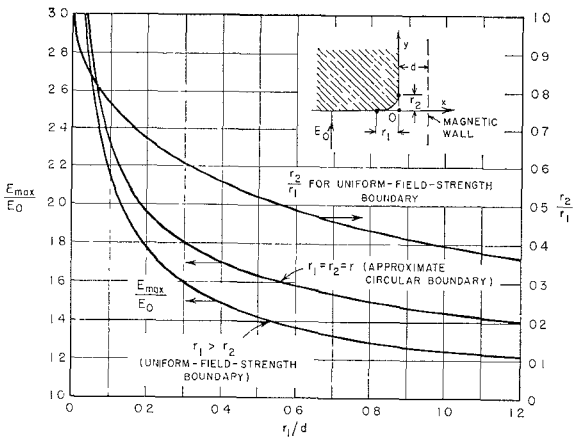

Fig. 11—Plot of E_{max}/E_0 for rounded 90-degree corner near a magnetic wall; also, r_2/r_1 for a uniform-field-strength boundary.

B. Constant-Field-Strength Boundary

The rounded 90-degree corner shape having constant field strength E_{max} on the curved portion of the boundary has been solved for the case of an adjacent magnetic wall [see Part B-2) of Appendix]. The curved-boundary end-point dimensions r_1 and r_2 are given by

$$\frac{r_1}{d} = \frac{1}{\pi}\left[\sqrt{\frac{1}{\lambda^2}-1} - \tan^{-1}\sqrt{\frac{1}{\lambda^2}-1}\right] \tag{7}$$

$$\frac{r_2}{d} = \frac{1}{\pi}\left[\tanh^{-1}\sqrt{1-\lambda^2} - \sqrt{1-\lambda^2}\right], \tag{8}$$

where λ is a parameter with value between 0 and 1. In terms of λ, the ratio of constant field strength E_{max} on the curved boundary to the distant uniform field E_0 is

$$\frac{E_{max}}{E_0} = \sqrt{\frac{1+\lambda}{1-\lambda}}. \tag{9}$$

The resulting curves of E_{max}/E_0 and r_2/r_1 are shown in Fig. 11. Note that the E_{max}/E_0 curve falls below the corresponding curve for the approximate circular-boundary case, as would be expected.

Detailed boundary curves for this case may be plotted from the following equations:

$$\frac{x}{d} = \frac{1}{\pi}\left\{\tan^{-1}\sqrt{u-1} - \sqrt{u-1}\right\} \tag{10}$$

$$\frac{y}{d} = \frac{1}{\pi}\left\{\tanh^{-1}\sqrt{1-\lambda^2 u} - \sqrt{1-\lambda^2 u}\right\}, \tag{11}$$

where λ is the same parameter as in (7), (8), and (9), u is a variable in the interval $1 \leq u \leq 1/\lambda$, and the coordinate system is as shown in Fig. 11. The boundary shapes yielded by (10) and (11) resemble those in Fig. 8 very closely, if the horizontal and vertical scale factors are altered to make the end points correspond to the appropriate values of r_1/d and r_2/d.

VI. Rounded 45-Degree Corner

The solution for a rounded 45-degree corner adjacent to an electric wall is outlined in Part C of the Appendix. This configuration and its symmetrical equivalent are shown in Fig. 2(b). The resulting curved boundary is neither a circular arc, nor a shape having constant field strength. For $r/b \ll 1$, the curve has the appearance shown in Fig. 12. The formula for this curve is

$$z = -\frac{r}{2^{5/4}}\left\{(t-1)^{5/4} + (t+1)^{5/4}\right\}, \qquad (12)$$

where $z = x + jy$ is a point on the curve with coordinate system as shown in Fig. 12, and t is a real variable in the interval $-1 \leq t \leq 1$. The field strength along the curved portion of the boundary is given, in the case $r/b \ll 1$, by

$$E(z) = \frac{(2+\sqrt{2})^{1/2} E_c}{\left[(1-t)^{1/2} + (1+t)^{1/2} + \sqrt{2}(1-t)^{1/4}(1+t)^{1/4}\right]^{1/2}} \qquad (13)$$

in which E_c is the field strength at the center point of the curve. Because of the assumption that $r/b \ll 1$, $E(z)$ is a symmetrical function of t near the corner. Eq. (13) is plotted in Fig. 13, where it is seen that the field strength on the boundary is almost constant except very near the junction points between curved and straight parts of the boundary. For $r/b \ll 1$, the ratio of field strength at the center of the curve to the uniform field strength in the parallel-plane region is

$$\frac{E_c}{E_0} = \frac{2}{(1+\sqrt{2})^{1/2}}\left(\frac{2}{5\pi}\right)^{1/5}\left(\frac{b}{r}\right)^{1/5} = 0.853\left(\frac{b}{r}\right)^{1/5}. \qquad (14)$$

Clearly, if the transitions from the curved-to-straight portions of the boundary were made slightly more gradual, the sharp rise at the junction points could be greatly reduced, with the maximum field strength on the boundary perhaps 1.1 times the value at the center of the curve.

Because of the one-fifth-root dependence in (14), the increase in E_c/E_0 is very slow relative to b/r. For example, $E_c/E_0 = 1.35$ when $r/b = 0.1$, while for $r/b = 0.01$, $E_c/E_0 = 2.14$. These are much smaller field-strength values than occur with 90-degree rounded corners.

VII. Conclusions

In high-power filters, whether operated with high internal pressure or vacuum, the power-handling ability is limited by electric-field concentrations at corners. By increasing the radius of curvature of these corners, the power rating of the filter may be increased. The formulas and graphs contained in this paper give quantitative data for various practical rounded-corner configurations. With these data, a filter designer can predict the power rating of a given structure or, if a particular rating is specified, he can select the necessary rounded-corner dimensions to meet that requirement.

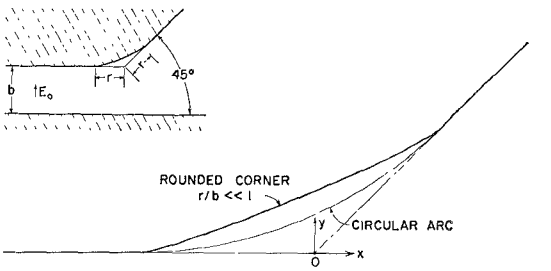

Fig. 12—Shape of rounded 45-degree corner drawn to scale for $r/b \ll 1$.

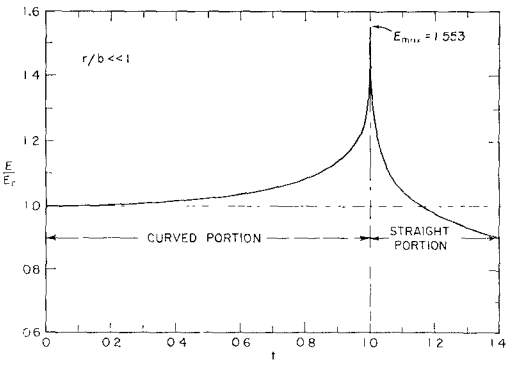

Fig. 13—Electric field strength on boundary of the rounded 45-degree corner shown in Fig. 12 (t is a "length" parameter measured from the center of the corner).

Some of the rounded corners considered in this paper are approximations to circular arcs, while others are shaped so that the electric field strength is uniform on the rounded portion of the boundary. The uniform-field-strength corners may be considered to be optimum, since any other boundary curve starting and ending at the same points would have a greater field strength somewhere on the curve.

Machining with high precision the exact theoretical shapes treated in this paper would not be a straightforward operation. Fortunately, minor deviations in shape will result in only small changes in the value of maximum field strength, as long as the boundary curve is smooth.

Appendix

A. Analysis of Array of 180-Degree Rounded Corners

Following a suggestion of Wheeler,[11] one may show that the periodic z-plane boundary in Fig. 14(a) is transformed into the real axis of the $w = u + jv$ plane in Fig. 14(b) by the following relation:

$$\frac{dz}{dw} = \sqrt{1 - m^2 \tan w} + jm \tan w, \qquad (15)$$

where m is a real constant between 0 and ∞. The single period of the z-plane boundary between $x = 0$ and $x = \pi$

maps into the u axis, also between 0 and π. Inspection of (15) shows that dz/dw is constant in magnitude but variable in angle for w real and in the range $|u| \leq \tan^{-1}(1/m)$. This range of u corresponds to the curved part of the z-plane boundary. The electric field strength in the z plane is proportional to $|dw/dz|$, and hence the field strength is constant along the curve. Further examination of (15) shows that this constant value of field strength is the maximum occurring in the cross section. Integration of (15) and substitution of the appropriate boundary conditions yields (1)—(4).

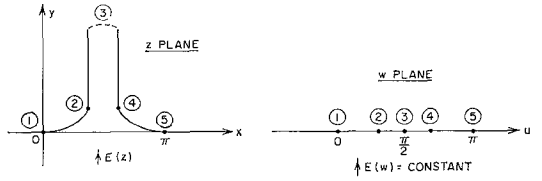

Fig. 14—Transformation for array of 180-degree rounded corners.

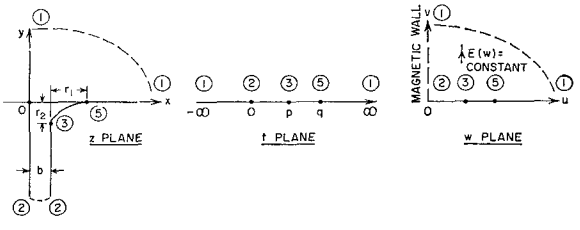

Fig. 15—Transformations for rounded 90-degree corner near magnetic wall.

B. Analysis of Rounded 90-Degree Corner Near Magnetic Wall

1) *Approximate Circular Boundary:* Weber[14] gives the following transformation (with notation changed) relating the z- and t-plane boundaries of Fig. 15:

$$\frac{dz}{dt} = \frac{C_1}{t}\left\{\sqrt{t-p} + \lambda\sqrt{t-q}\right\}, \tag{16}$$

where C_1, p, q, and λ are real, positive constants, with $q>p$. The formula for z is obtained by integration. Relations between p, q, and λ are established such that $r_1=r_2=r$. These constants may be computed from his formulas as functions of r/b, or read from his graph.[20] Weber applied this transformation to the case of an electric-wall boundary adjacent to the rounded corner by assuming the real axis of the t plane to be an electric wall with a discontinuity in potential at point 2. However, the same transformation may be used for an adjacent magnetic wall by transforming the t plane into the w plane as shown in Fig. 15. The vertical magnetic wall in the w plane maps into the adjacent magnetic wall of the z plane. Since the electric field in the upper-right-hand corner of the w plane is uniform, the electric field strength in the z plane is proportional to $|dw/dz|$, and was found to be

$$E(z) \propto \frac{1}{\left|\sqrt{1-\frac{p}{t}} + \lambda\sqrt{1-\frac{q}{t}}\right|}. \tag{17}$$

From this, (6) for E_{max}/E_0 was derived.

2) *Constant-Field-Strength Boundary:* Inspection of (17) shows that if λ is set equal to $\sqrt{p/q}$, $E(z)$ will be constant for t real and in the interval $p \leq t \leq q$. When $\lambda=\sqrt{p/q}$ is substituted in (17) and in Weber's formulas, (7)—(11) result.

C. Analysis of Rounded 45-Degree Corner

By application of the Schwartz-Christoffel method, the z-plane boundary in Fig. 16(a) was transformed into the real axis of the t plane by the following relation:

$$\frac{dz}{dt} = \frac{Ct^{1/4}}{t-p}. \tag{18}$$

After integration and substitution of boundary conditions, the following formula for z as a function of t was obtained:

$$z = z(t) = \frac{1+j}{\pi} b\left\{2\sqrt{2}\left(\frac{t}{-p}\right)^{1/4} - \ln\left[\frac{\left(\frac{t}{-p}\right)^{1/2} + 1 + \sqrt{2}\left(\frac{t}{-p}\right)^{1/4}}{\left(1+\frac{t}{-p}\right)^{1/2}}\right] - \tan^{-1}\left[\frac{\sqrt{2}\left(\frac{t}{-p}\right)^{1/4}}{1-\left(\frac{t}{-p}\right)^{1/2}}\right]\right\}, \tag{19}$$

where p is a positive constant. This transformation yields an abrupt 45-degree corner. To round the corner as in Fig. 16(b), (19) was modified into the following form:

$$z = Az(t') + (1-A)z(t''), \tag{20}$$

where

$$t' = \left(\frac{p+\delta_1}{p}\right)t - \delta_1 \text{ and } t'' = \left(\frac{p-\delta_2}{p}\right)t + \delta_2. \tag{21}$$

The changes in variable of (21) are such that $t'=t''=t$ at the critical points $t=1$ and ∞, but not at $t=0$. At $t'=0$, $t=p\delta_1/(p+\delta_1)$, while at $t''=0$, $t=-p\delta_2/(p-\delta_2)$. As a result of this modification, a gradual change of slope from 0 to 45 degrees occurs with (20) for t in the range $-\delta_2/(1-\delta_2) \leq t \leq \delta_1/(1+\delta_1)$.

[20] Weber, *op. cit.*, p. 375.

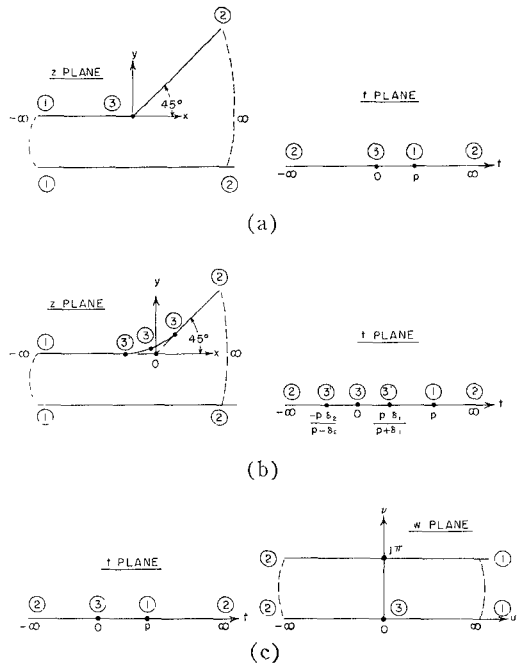

Fig. 16—Transformations for 45-degree corner. (a) Abrupt 45-degree corner. (b) Rounded 45-degree corner. (c) Transformation between t and w planes.

The procedure to follow in determining the contants A, δ_1, and δ_2 for a given value of r/b is to let (20) take on the following values:

$$z = -r \quad \text{when} \quad t' = 0 \quad \text{and} \quad t'' = \frac{p(\delta_1 + \delta_2)}{p + \delta_1} \tag{22}$$

$$z = \frac{1+j}{\sqrt{2}} r \quad \text{when} \quad t' = \frac{p(\delta_1 + \delta_2)}{p - \delta_2} \quad \text{and} \quad t'' = 0. \tag{23}$$

Since these are only two conditions and there are three constants to be determined, one additional condition may be specified. This could be, for example, that the curve should be most nearly symmetrical about its center point.

The case $r/b \ll 1$ is of particular practical interest. In the limit $r/b \to 0$, the constants have values $A = 1/2$ and $\delta_1 = \delta_2 = \delta$, so that δ becomes the only unknown. Furthermore $\delta \ll p$ so that (20) and (21) become

$$z = \tfrac{1}{2} z(t - \delta) + \tfrac{1}{2} z(t + \delta). \tag{24}$$

In the limit $t \to 0$, (19) and (24) reduce to

$$z = -\frac{2b}{5\pi p^{5/4}} \left\{ (t - \delta)^{5/4} + (t + \delta)^{5/4} \right\}. \tag{25}$$

Eq. (25) may be used to calculate the shape of the z-plane boundary in the vicinity of the rounded corner, but it does not, of course, yield the adjacent electric wall.

A discontinuity in potential occurs at point 1 in the z and t planes, so that the electric field in the t plane is nonuniform. The real axis of the t plane may be transformed into the w-plane boundary of Fig. 16(c) containing a uniform electric field by means of this differential relation

$$\frac{dw}{dt} = \frac{1}{p - t}. \tag{26}$$

The electric field within the z-plane boundary near the corner may then be obtained by differentiation of (23) and combination with (26), with $|t| \ll p$,

$$E(z) \propto \left| \frac{dw}{dz} \right| = \frac{2\pi p^{1/4}/b}{\left| (t - \delta)^{1/4} + (t + \delta)^{1/4} \right|}. \tag{27}$$

The uniform field E_0 far from the corner is obtained from (18) and (26) with $t \to p$ and $C = -b/\pi p^{1/4}$

$$E_0 \propto \left| \frac{dw}{dz} \right| = \frac{\pi}{b}. \tag{28}$$

Combination of (27) and (28) gives the following formula for $E(z)/E_0$ valid in the vicinity of the rounded corner for the case $r/b \ll 1$:

$$\frac{E(z)}{E_0} = \frac{2p^{1/4}}{\left| (t - \delta)^{1/4} + (t + \delta)^{1/4} \right|}. \tag{29}$$

The maximum-field-strength points occur at $t = \pm\delta$. At $t = \delta$, (25) yields

$$r = \frac{2b}{5\pi p^{5/4}} (2\delta)^{5/4} \quad \text{and} \quad p^{1/4} = \left(\frac{2b}{5\pi r} \right)^{1/5} (2\delta)^{1/4}. \tag{30}$$

Eqs. (12)–(14) now follow readily from (25), (29), and (30), when δ is set equal to unity.